

## Sonic characterization of porous $\text{Si}_3\text{N}_4$ produced by various pore formers

G. Topateş<sup>a,\*</sup>, E. Eren Gültekin<sup>b</sup>

<sup>a</sup> Çan Vocational College, Çanakkale Onsekiz Mart University, 17400, Çanakkale, Turkey

<sup>b</sup> Department of Ceramic and Glass Design, Nevşehir Hacı Bektaş Veli University, 50800, Nevşehir, Turkey

\* Corresponding e-mail address: topatesates@gmail.com

Received 16.12.2013; published in revised form 01.03.2014

### ABSTRACT

**Purpose:** Study aims to investigate the elastic properties of porous  $\text{Si}_3\text{N}_4$  thus three different starch type as pore former additives were used to obtain different pore characteristics.

**Design/methodology/approach:** Porous  $\text{Si}_3\text{N}_4$  ceramics were fabricated by partial sintering and pore former addition. Pore formers consisted of elliptic, round and angular particles were used. Elastic, shear and bulk moduli of the samples were measured by ultrasonic measurement using ultrasonic A-scan.

**Findings:** Starches whose particles are isometric and angular lead to higher elastic properties thus it's possible to tailor the elastic properties by using pore formers with different morphologies. Starches whose particles are isometric and angular lead to higher elastic properties thus it's possible to tailor the elastic properties by using pore formers with different morphologies

**Research limitations/implications:** The porosity of fabricated ceramics varied between 50-70% and pore size were restricted to around 1  $\mu\text{m}$  as a result of a small grain width of beta- $\text{Si}_3\text{N}_4$  grains and interlocking structure formed by these grains.

**Practical implications:** The Young's (elastic) modulus of sample without pore former was 30 and it decreased to 10-17 GPa by using different pore formers. Same trend also observed for shear modulus.

**Originality/value:** Even though using similar size and same amount of pore former, slight differences were observed as a result of different geometry of pore former particles and hence pore geometry.

**Keywords:** Ceramics and glasses; Mechanical properties; Porous  $\text{Si}_3\text{N}_4$ ; Starch; Sonic measurement

**Reference to this paper should be given in the following way:**

G. Topateş, E. Eren Gültekin, Sonic characterization of porous  $\text{Si}_3\text{N}_4$  produced by various pore formers, Journal of Achievements in Materials and Manufacturing Engineering 63/1 (2014) 13-18.

### PROPERTIES

## 1. Introduction

$\text{Si}_3\text{N}_4$  ceramics have become at the forefront among the porous ceramics owing to their superior mechanical properties (Miyakawa, 2003, Yang, 2002, Yang, 2003). Despite elastic properties dramatically decrease with increasing porosity amount, porous  $\text{Si}_3\text{N}_4$  ceramics possess sufficient strength. It's possible to machine  $\text{Si}_3\text{N}_4$  ceramics as a result of low moduli values (especially Young's modulus) combining with sufficient strength (Kawai, 1998). Therefore, characterizing the elastic properties has great importance for post-sintering steps. Several techniques have been used to measure the elastic properties and among them nondestructive testing (NDT) is an evaluation performed on an object of any type, size, shape or material without changing or altering that object in any way to determine the presence or absence of discontinuities, or to evaluate other material characteristics. One of the widespread used NDT methods is ultrasonic test method which has principles: high-frequency sound pulses from a transducer propagate through the test material, reflecting at interfaces. For sound waves in solids, liquids and gases the vibrating bodies are the particles making up the substance and restoring forces are the elastic bonds holding the substance together.

Audible sound is an example of a vibration mode called a 'compression/longitudinal wave'. It travels from the source by a succession of shunting actions from one particle to the next. Each particle vibrates at the frequency of sound. As each particle oscillates, it squashes the 'spring' to the next neighbor and starts the neighbor oscillating. As the oscillation passes from one particle to the next, and the next, and so on, the sound wave is said to travel or propagate through the material. Compression wave can exist in solids, liquids or gasses. Other modes of vibration can exist, but only in solids. The various ways in which sound can propagate are usually described in terms of the direction of particle motion in relation to the direction in which the sound wave travels. Compression waves can be defined on this basis as waves in which the particle motion is in the same plane as the direction of propagation. All three media have forces that bind the particles together to resist squashing or pulling apart (compression or tension). In solids, this is provided by the modulus of elasticity, known as 'Young's modulus of elasticity'.

Solids, unlike liquids and gasses, also have rigidity that is a resistance to shear loads. It is the rigidity that has to be overcome when snapping a stick, for instance. The name for this resistance to shear loads in solids is called the modulus of rigidity (shear modulus) and it allows sound to propagate in a different way under certain circumstances. This new

mode of propagation is known as a shear/transverse wave and is defined as a wave in which the particle motion is at right angles to the direction of propagation.

Sound travels at different speeds through different materials. Shear waves do not travel at the same velocity as the compression wave in a given material. This is because it is the modulus of rigidity, rather than Young's modulus, that dictates the velocity, and the modulus of rigidity is lower than the modulus of elasticity. This means that the shear wave velocity is always slower than compression wave velocity in a material (Hellier, 2001). The velocity of ultrasonic waves in fluids and solids, with the attendant effect on the beam at interfaces, depends upon factors such as ambient pressure, density, the ratio of specific heats, bulk modulus, Young's modulus and other mechanical properties (Haran, 1979).

The effect of porosity on elastic properties has been studied since 1950. Understanding this relationship is important because these materials are mainly produced by powder technology routes and usually have a fraction of involuntary residual porosity, a characteristic which degrades mechanical properties. Moreover, the production of new and reliable porous materials for catalytic supports and filters depends on the optimization of mechanical properties (Yoshimura, 2007). Beside porosity, pore characteristics such as pore size, its distribution and morphology are the effective parameters on the elastic properties. Study aims to investigate the elastic properties of porous  $\text{Si}_3\text{N}_4$  thus three different starch type as pore former additives were used to obtain different pore characteristics.

## 2. Description of the approach, work methodology, materials for research, assumptions, experiments

### 2.1. Materials processing

$\beta$ - $\text{Si}_3\text{N}_4$  powder (Silzot HQ, Germany with  $d_{50}=2.0\ \mu\text{m}$ ) as  $\text{Si}_3\text{N}_4$  source and  $\text{CaCO}_3$  (Riedel-de Haen, Germany) as sintering additive with amount of 1.44 wt. % were used. Three different starch type; wheat, potato and corn (Gunes Nisasta) were preferred as pore former additives. SEM images (Zeiss Evo 50 EP @ Anadolu University) of all starches were given in (Figs. 1a and c). Using starch as a pore former brings some advantages such as simple-low cost process, improved green strength and producing non-toxic materials during burn-out (Gregorova, 2007).

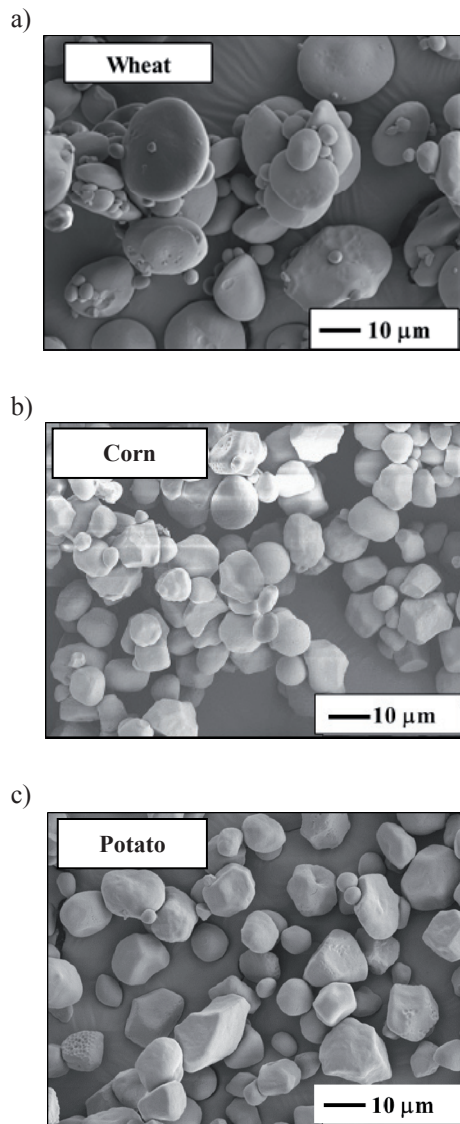


Fig. 1. SEM images of starches a) Wheat, b) Corn and c) Potato

According to SEM images, wheat starch has round and elliptic particles with wide particle size distribution and they tend to agglomerate. The morphology of both potato and corn starch is nearly same. They contain isometric and angular particles but the particle size of corn is relatively higher than that of potato. The starch content varied between 0 to 30 vol. % for wheat addition and they were denominated as SN-0 to SN-30W. For potato and corn starch, the amount of addition was fixed to 20 vol. % and they were referred as SN-20P and SN-20C, respectively. The mixture of  $\beta$ -powder and  $\text{CaCO}_3$  was milled by

planetary mill (Fritsch Pulverisette 5 @Anadolu University) using deionized water at 100 rpm for 1 h. Starches were added to the powder mixtures by means of dry method to prevent swelling of starch particles. Ball milling was done for 1 h by using LD-PE jars to obtain homogenous mixing of powder and starch. Uniaxial dry pressing was used for shaping samples' diameter was 20 mm and thickness was 10 mm. Starch removal was performed under air at 600°C for 1 h. Pressureless sintering was applied by a graphite furnace (Thermal Technology, LLC @Anadolu University) at 1750°C for 5 h under  $\text{N}_2$  atmosphere applying 10°C/h heating rate. Porosity of samples was measured via Archimedes' displacement method. Mercury porosimeter (Quantachrome PoreMaster-60 @Anadolu University) was performed to characterize pore size and distribution of samples.

## 2.2. Sonic measurement

Olympus Panametrics Model 5800 Computer Controlled Pulser/Receiver (pulse-echo method, A-scan) was used for ultrasonic characterization of samples. The transducers' center frequencies were 5 MHz for longitudinal waves and 2.25 MHz for transverse waves which were connected to the device for transmitting the ultrasonic waves to the sample. The propagation time of ultrasonic wave measurements as a result of ultrasonic signals of the inspected samples with the transducer was performed using a digital oscilloscope (Tektronix TDS 1012 Two Channel Digital Storage Oscilloscope). This analysis was repeated five samples for each composition. The ultrasonic wave's propagation time was determined to within an accuracy of  $\pm 40$  ns. The thickness of the samples was measured with a micrometer (0.01 mm resolution Fowler IP 54 micrometer). The velocity of the waves through the thickness of the samples was determined by Eq. 1 (Medding, 1996):

$$V=(2xd)/t \quad (1)$$

Here, d: sample thickness (mm), t: ultrasonic wave's propagation time (ns) and V: ultrasonic wave's propagation time (m/s) (Medding, 1996). Assuming that the samples used in this analysis are isotropic, standard velocity-elasticity relationships can be used to calculate the Young's, shear, bulk modulus. These relationships are:

$$E= [v_l^2 \rho (1+ \sigma)(1-2\sigma)] / (1- \sigma) \quad (2)$$

$$G= v_s^2 \rho \quad (3)$$

$$K=E/[3(1-2\sigma)] \quad (4)$$

$$\sigma=(1-2b^2)/(2-2b^2) \quad (5)$$

where  $v_l$  is the longitudinal wave velocity (m/s),  $v_s$  the shear wave velocity (m/s),  $E$  the Young's modulus (pascals),  $G$  the shear modulus (pascals),  $K$  the bulk modulus (pascals),  $\sigma$  the Poisson's ratio and  $b = v_s / v_l$  (Kulkarni, 1994).

### 3. Description of achieved results of own researches

#### 3.1. Pore characteristics and microstructure of samples

Bulk density and apparent porosity of samples were listed in Table 1. The apparent porosity was increased from 52.3 to 72.5% for samples contain wheat starch. Equal apparent porosity values obtained for samples that have same amount but different types of starch. So, it will be reliable to determine the effect of pore characteristics on the elastic properties.

Secondary electron images of all samples were given between Figs. 2a)-f). Characteristic grain morphology of  $\beta$ - $\text{Si}_3\text{N}_4$  was obtained. All samples consisted of elongated and rod-like grains. Since the random distribution of these grains, an interlocking structure was formed for all samples. The effect of starch addition is very obvious from

the SEM images. The arrows show the pores formed after burning-out of starch. With increasing wheat starch, larger pore channels formed but the distribution of them was irregular. Any significant effect of starch type on the microstructure wasn't observed.

Table 1.

Bulk density and apparent porosity of samples

Sample	Bulk density, $\text{g}/\text{cm}^3$	Apparent porosity, %
SN-0	1.5	52.3
SN-10W	1.4	56.8
SN-20W	1.2	62.8
SN-30W	0.9	72.5
SN-20C	1.2	63.5
SN-20P	1.2	62.9

Figure 3 shows pore size and distribution of SN-20W, SN-20P and SN-20C. Owing to larger particle size distribution of wheat starch, SN-20W has bimodal pore size distribution. Its median pore size values are 1.5 and 2.5  $\mu\text{m}$ , respectively. Nearly same pore size values were obtained for SN-20P and SN-20C with a median value of 2  $\mu\text{m}$ . To sum up, any important distinction was not observed in the pore size distribution depending on the starch type.

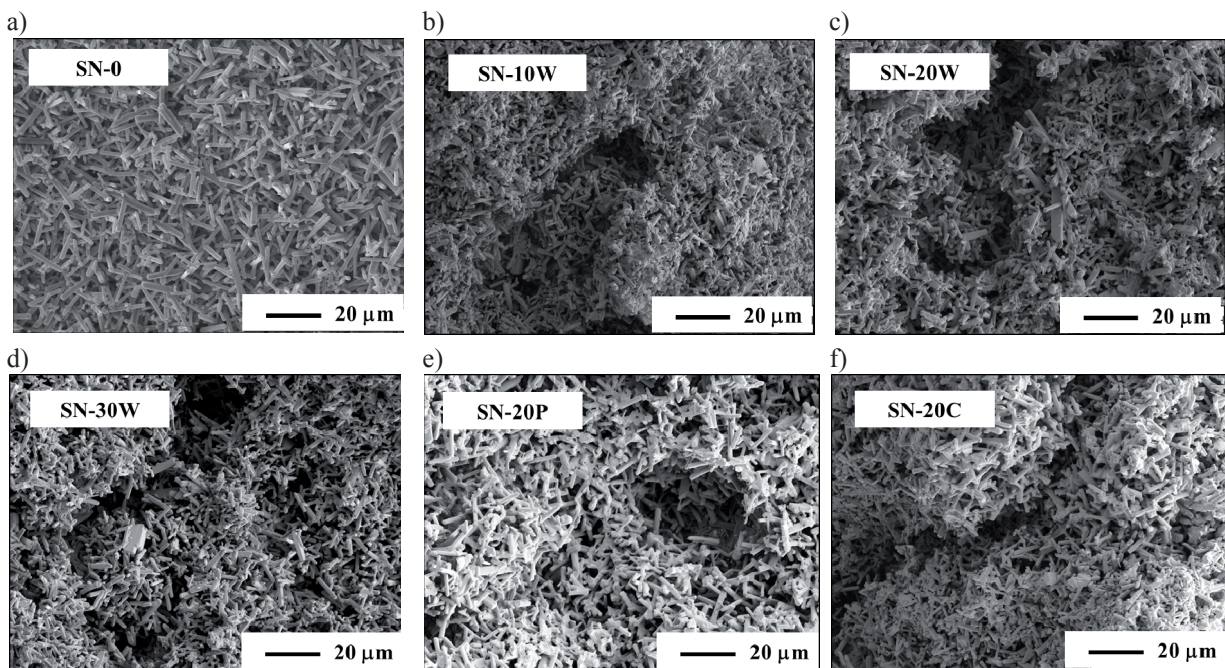


Fig. 2. SEM images of samples a) SN-0, b) SN-10W, c) SN-20W, d) SN-30W, e) SN-20P and f) SN-20C

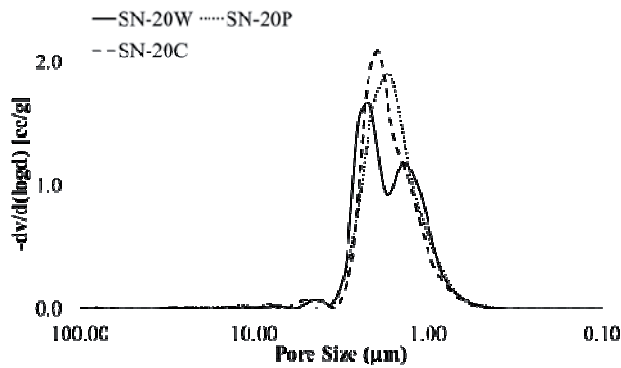


Fig. 3. Pore size distribution of SN-20W, SN-20P and SN-20C

### 3.2. Young's, shear and bulk moduli of samples

Longitudinal and shear sonic velocity values of samples were given in Table 2. When the amount of wheat starch content increases, the bulk density decreases and the apparent porosity increases. The porosity blocks the ultrasonic waves' propagation and decreases the ultrasonic wave velocity. As the starch content increases from 0 to 30%, apparent porosity increases; ultrasonic velocities decrease. Higher velocities were measured for SN-20P and SN-20C compare to SN-20W.

Table 2. Longitudinal and shear sonic velocity values of samples

Sample	$v_{\text{longitudinal}}$ , m/s		$v_{\text{shear}}$ , m/s	
	Average	Standard deviation, $\pm$	Average	Standard deviation, $\pm$
SN-0	4727.97	197.96	2862.30	177.74
SN-10W	4456.27	147.78	2381.62	67.81
SN-20W	3537.98	265.89	1878.92	120.63
SN-30W	1769.71	277.14	1083.18	23.70
SN-20C	4097.27	188.65	2069.48	86.02
SN-20P	4298.73	188.09	2392.09	86.47

Table 3 shows all elastic properties. Sample without starch the obtained Young's modulus value was 30 GPa and it reduced to 2.8 GPa with 30 vol.% wheat starch addition. For the same amount of starch addition, higher modulus values were achieved for SN-20P and SN-20C than SN-20W as given in Table 3. The porosity and pore

size values of all three samples were nearly same, however, their modulus values are different. Samples prepared by isometric and angular starch particles (potato and corn) have higher modulus than that of wheat.

Table 3. Elastic properties of samples

Sample	Young's modulus, GPa	Bulk modulus, GPa	Shear modulus, GPa
SN-0	30.2	17.4	12.5
SN-10W	20.2	16.9	7.8
SN-20W	10.3	8.5	4.0
SN-30W	2.8	1.6	1.2
SN-20C	13.4	13.1	5.1
SN-20P	17.2	12.8	6.7

Several studies have been carried out to characterize elastic properties of  $\text{Si}_3\text{N}_4$  and the results from these studies were compiled in Table 4. The Young's modulus values changes from 330 GPa to 60 GPa values depending on production procedure and porosity values.

Table 4. Young's and Shear moduli values of porous  $\text{Si}_3\text{N}_4$  obtained from previous studies (PHP: partial hot pressing, PFA: pore former addition, PS: partial sintering)

Material-reference	Production technique	Results	
		Porosity/ Pore size % / $\mu\text{m}$	Elastic properties, GPa
$\text{Si}_3\text{N}_4$ (5 wt.% $\text{Y}_2\text{O}_3$ ) -Yang, 2002	PHP-1800°C	0-30 %/ 0.1-1 $\mu\text{m}$	E=130-330
$\text{Si}_3\text{N}_4$ (6 wt.% $\text{Y}_2\text{O}_3$ +2 wt.% $\text{Al}_2\text{O}_3$ ) -Diaz, 2004	PFA-1800°C	0-25 %/ 0.5-40 $\mu\text{m}$	E=160-332
$\text{Si}_3\text{N}_4$ (6 wt.% $\text{Y}_2\text{O}_3$ +2 wt.% $\text{Al}_2\text{O}_3$ ) -Diaz, 2005	PS/PFA/PH P-1500-1800°C	2.3-35%/ N/A	E=60-310 G=40-120
$\text{Si}_3\text{N}_4$ (6 wt.% $\text{Y}_2\text{O}_3$ +2 wt.% $\text{Al}_2\text{O}_3$ ) -Redington, 2002	PS/PFA-1800°C	0-30 %/ N/A	E=180-330

Since the porosity values in the previous studies were considerably higher than the values obtained in this study, the Young's modulus and porosity values of samples contain wheat starch were plotted and fitted to an equation in Fig. 4 to estimate the Young's moduli where the porosity is 0. The calculated value is 320 GPa at zero porosity and it is consistent with the values given in Table 4.

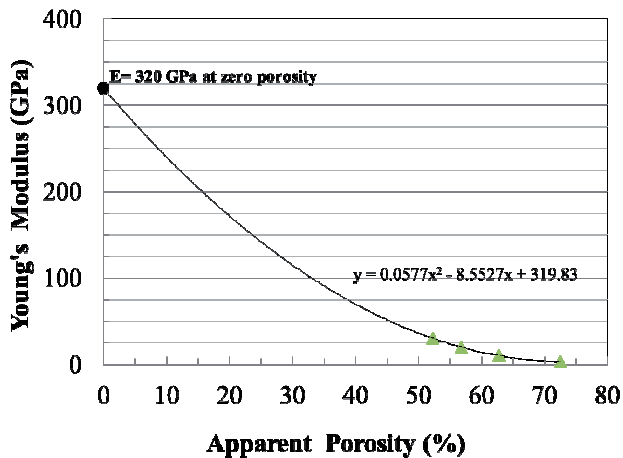


Fig. 4. Young's moduli against apparent porosities of samples produced with wheat starch

$\text{Si}_3\text{N}_4$  ceramic with higher porosity were produced via various type of starch addition and their elastic properties were characterized by ultrasonic measurement. Elastic properties were reduced by increasing porosity values. The estimated Young's modulus showed a good agreement with the literature values. Starches whose particles are isometric and angular lead to higher elastic properties thus it's possible to tailor the elastic properties by using pore formers with different morphologies. Further image analysis studies of pore structure of samples will be carried to prove the effect of the morphology of pore former on the elastic properties.

## Acknowledgements

All of the experimental studies were carried out at Anadolu University, Department of Materials Science and Engineering. The authors would like to thank to Department of Materials Science and Engineering.

## References

- [1] A. Diaz, S. Hampshire, Characterisation of porous silicon nitride materials produces with starch, *Journal of the European Ceramic Society* 24 (2004) 413-419.
- [2] A. Diaz, S. Hampshire, J.F. Yang, T. Ohji, S. Kanzaki, Comparison of mechanical properties of silicon nitrides with controlled porosities produces by different fabrication routes, *Journal of the American Ceramic Society* 88 (2005) 698-706.
- [3] E. Gregorova, W. Pabst, Porosity and pore size control in starch consolidation casting of oxide ceramics – achievements and problems, *Journal of the European Ceramic Society* 27 (2007) 669-672.
- [4] M.E. Haran, Visualization and measurement of ultrasonic wavefronts, *Proceedings of the IEEE* 67/4 (1979) 454-466.
- [5] C.J. Hellier, *Handbook of Nondestructive Evaluation*, Mc Graw-Hill, New York, 2001, 1.1-7.10.
- [6] C. Kawai, A. Yamakawa, Machinability of high strength porous silicon nitride ceramics, *Journal of the Ceramic Society of Japan* 106 (1998) 1135-1137.
- [7] N. Kulkarni, B. Moudgil, M. Bhardwaj, Ultrasonic characterization of green and sintered ceramics: I, time domain, *American Ceramic Society Bulletin* 73 (1994) 146-153.
- [8] J.A. Medding, Nondestructive evaluation of zirconium phosphate bonded silicon radomes, Master Thesis, Virginia Polytechnic Institute and State University, 1996, Virginia, 43.
- [9] N. Miyakawa, H. Sato, H. Maeno, H. Takahashi, Characteristics of reaction-bonded porous silicon nitride honeycomb for DPF substrate, *Journal of Society of Automotive Engineers Review* 24/3 (2003) 269-276.
- [10] W. Redington, J. Lonergan, G. Gonidec, A. Diaz, H. Bilgen, S. Hampshire, Controlled porosity in silicon nitride, *Materials Science Forum* 383 (2002) 19-24.
- [11] J.F. Yang, T. Ohji, S. Kanzaki, A. Diaz, S. Hampshire, Microstructure and Mechanical Properties of Silicon Nitride Ceramics with Controlled Porosity, *Journal of the American Ceramic Society* 85 (2002) 1512-1516.
- [12] J.F. Yang, Z.Y. Deng, T. Ohji, Fabrication and characterisation of porous silicon nitride ceramics using  $\text{Yb}_2\text{O}_3$  as sintering additive, *Journal of the European Ceramic Society* 23/2 (2003) 371-378.